

One-dimensional models and thermomechanical properties of solidsPaolo De Gregorio,^{1,2,*} Lamberto Rondoni,^{1,2} Michele Bonaldi,^{3,4} and Livia Conti⁵¹*Dip. di Matematica, Politecnico di Torino, Corso Duca degli Abruzzi 24, I-10129 Torino, Italy*²*INFN, Sezione di Torino, Via P. Giura 1, I-10125 Torino, Italy*³*Institute of Materials for Electronics and Magnetism, Nanoscience-Trento-FBK Division, I-38123 Povo, Trento, Italy*⁴*INFN, Gruppo Collegato di Trento, Sezione di Padova, I-38123 Povo, Trento, Italy*⁵*INFN, Sezione di Padova, Via Marzolo 8, I-35131 Padova, Italy*

(Received 7 April 2011; revised manuscript received 16 November 2011; published 12 December 2011)

We use open-ended chains of oscillators, like those introduced by Fermi, Pasta, and Ulam, to mimic thermomechanical properties of crystalline solids, such as thermal expansion and the change of elasticity and quality factors with temperature. We employ molecular dynamics and theoretical arguments, separately. Features of real solids are reproduced, such as the positiveness of the coefficient of thermal expansion and the decrease of the modulus of elasticity and of the quality factor with temperature. The results depend strongly on the interparticle potential at energy levels much higher than the average energy of the chain, with the Lennard-Jones potential yielding the most realistic cases.

DOI: [10.1103/PhysRevB.84.224103](https://doi.org/10.1103/PhysRevB.84.224103)

PACS number(s): 62.20.D-, 05.10.-a, 05.20.-y

I. INTRODUCTION

Fermi-Pasta-Ulam (FPU) models¹ are linear chains of interacting particles providing a minimal framework for studies of ergodicity, dynamical relaxation, and diffusion laws with given interparticle potentials, initial conditions, and boundary conditions.²⁻⁴ In contrast, three-dimensional models,⁵ sometimes complemented by secondary relations of either thermodynamic origin or derived by ensemble theory of large systems,^{6,7} were developed to evaluate structural and dynamical properties of specific solids from the interparticle potential. Here we investigate whether the conceptually simple FPU framework suffices in modeling the qualitative behavior of thermomechanical properties of solids, such as elastic modulus, thermal expansion, and mechanical losses. We also study how this behavior is related to the interparticle potential, gaining considerable insight into thermally induced softening of materials.

We consider a chain of oscillators with one free end to study the variations of its length in response to an external force or to temperature changes, both from theoretical considerations and by direct access to the quantities of interest in simulations. We consider different asymmetric potentials and require that the atoms make only small vibrations around their equilibrium positions. Note that the use of an open-ended chain prevents mechanical internal stress induced by the thermal expansion and mimics the most common experimental conditions. This choice of boundary condition has been considered before only in a few works on heat conduction² and FPU's recurrence effects.⁸

When subjected to a temperature increase, most solids expand with a characteristic rate expressed by a (usually positive) coefficient of thermal expansion.⁹ Concurrently small stresses and strains are proportional (Hooke's law). The proportionality constants are termed collectively modulus of elasticity; most commonly one refers to the Young's elasticity modulus E , which is the ratio of tensile stress to tensile strain. In most cases, Young's modulus decreases with increasing temperature, often linearly over an extended range.¹⁰⁻¹² Experiments and qualitative theoretical arguments have led to a

formula for Young's modulus of many crystalline solids,¹³⁻¹⁵ which has recently been related to bonding energetics,¹⁶ of the form

$$E = E_0 - bT \exp(-T_0/T). \quad (1)$$

In the large- T limit, a linear decrease of E with T can thus be observed. Equation (1) and the thermodynamical arguments of Ref. 17 agree on the experimental finding that E approaches E_0 from below with a vanishing slope in the $T \rightarrow 0$ limit. This quantum mechanical effect is not reproduced by our classical models. Conversely, our theory is consistent with the observed behavior at higher temperatures.

II. THE MODEL

Our model consists of N identical particles in one line interacting with each other's nearest neighbors and obeying Newtonian dynamics. Particle number 1 interacts with particle 2 on one side, and with a wall on the opposite side. The N th particle of the chain is the furthest from the origin at all times, defining its coordinate as the total length. If the interaction potential is a perturbed harmonic potential, we have a low-energy FPU-like model with asymmetric boundary conditions.

We perform our analysis with three interaction potentials (see inset of Fig. 1): the Lennard-Jones (LJ) potential

$$V_{\text{LJ}}(x) = \epsilon(x^{-12} - 2x^{-6}) \quad (2)$$

and the truncated series expansion V_t

$$V_t(x) = h[(x-1)^2 - \lambda(x-1)^3 + \mu(x-1)^4], \quad (3)$$

with two distinct sets of parameters λ and $\mu \geq 0$. Differently from most FPU models, we consider the odd power of x to have a negative sign to mimic an asymmetric potential with short-range repulsion and long-range attraction. The series expansion of the LJ potential around the minimum R_0 has indeed alternating signs. We take $x = \frac{r}{R_0}$, where r is the distance between any two (nearest-neighbor) interacting atoms and $r = R_0$ at $T = 0$; h is an energy parameter, stemming from a reference microscopic harmonic constant of $2h/R_0^2$.

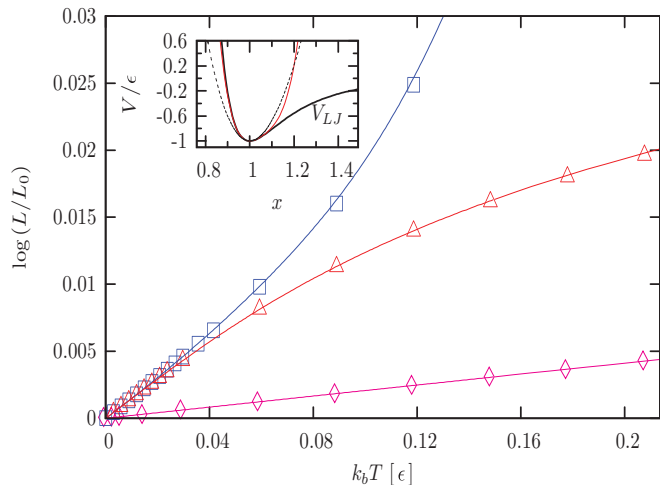


FIG. 1. (Color online) Thermal expansion data for V_{11} (\diamond), V_{12} (\triangle), and V_{LJ} (\square). The temperature is expressed in units of the energy ϵ . The solid lines are evaluated according to Eq. (6). Inset: LJ interaction potential V_{LJ} (thick solid line), V_{11} (dashed line), and V_{12} (thin solid line, red online).

Our values for λ and μ imply that $V_i(x)$ has one minimum at $x = r/R_0 = 1$. All these potentials are asymmetric; that is, the restoring force toward R_0 is stronger at short distances ($r < R_0$) than at large distances ($r > R_0$). Because the chain is open at one end, the effect of the asymmetry at temperatures $T > 0$ is a lengthening with respect to the $T = 0$ length ($L_0 = NR_0$) obtained for all particles in the minima of the potential. These potentials are defined as functions of the distance r between two particles which are nearest neighbors, differently from typical FPU models where they are defined in terms of the coordinate difference between two particles which start as nearest neighbors.

The confining potential of Eq. (3) prevents the breaking of the chain, while for a $V(x)$ that vanishes in the $x \rightarrow \infty$ limit, such as V_{LJ} , a rare fluctuation of local relative velocities (in opposite directions) may lead the chain to break at one or more points. As we shall discuss, this effect is inevitable in the large N , $t \rightarrow \infty$ limit, but is not observed in practice if the temperature is very low. Whenever the LJ system becomes unstable, at high energies, we apply strategies like the one detailed further below. In most FPU-type models, the two ends are held in their positions at a distance $L_0 = NR_0$. This avoids breaking of the chain but rules out thermal expansion.

In order to have the harmonic coefficients of the series expansions coincide, we set $h = 36\epsilon$ all throughout. We begin with $\lambda = \mu = 1$, similarly to common cases in the literature, where $|\lambda|$ and $|\mu|$ are of order unity. In the second case, we compared with the LJ model. A truncated expansion around $x = 1$ ($r \simeq R_0$) of V_{LJ} leads to Eq. (3) with $\lambda = 7$, $\mu = 53\lambda/12$. In the following, we shall call V_{11} and V_{12} the potential described by the truncated expression (3) with parameters $\lambda = \mu = 1$ and with $\lambda = 7$, $\mu = 53\lambda/12$, respectively.

In simulations, to represent a system at constant temperature, we supplemented the Hamiltonian equations of motion with a Nosé-Hoover thermostat. To compute the resonance frequency and the quality factor, we opted for simulations at

constant energy. The corresponding equations of motion read:

$$m\ddot{r}_i = -\frac{\partial W(|r_i - r_{i+1}|)}{\partial r_i} - \frac{\partial W(|r_i - r_{i-1}|)}{\partial r_i} - \chi\dot{r}_i, \quad (4)$$

$$\dot{\chi} = \frac{m}{\tau^2} \left(\frac{K}{k_B T} - 1 \right), \quad K(t) = \frac{m}{N} \sum_{j=1}^N \dot{r}_j(t)^2,$$

where $i = 1, \dots, N$, $r_{N+1} \equiv r_N + R_0$, and we mainly used $N = 128$. $W(r) = V(xR_0)$. $\chi(t)$ is the dynamical variable driving the energy exchanges with the thermal bath, τ is a characteristic time of the bath, which we set to 10 times the simulation time step of 10^{-14} s. m is the mass of each particle and $K(t)$ is the instantaneous average kinetic energy, which the bath forces to fluctuate around the chosen value $k_B T$. If we take $m = 1$ u and $R_0 = 1$ Å as a reference, then $\epsilon = 1.37 \times 10^{-21}$ J. Here we express both the energy and K (hence the “kinetic” temperature $k_B T$) in units of the LJ potential energy depth ϵ . Often, in one-dimensional FPU simulations, m and R_0 are rather set to be dimensionless and equal to unity. This would translate into $\epsilon = 82.78$ and $h = 2980$. In various instances, we explored sizes up to $N = 512$, finding no quantitative differences with the case $N = 128$ for the correctly normalized quantities, except for finite-size effects consistent with physical principles. The agreement with the theory, where we can make comparisons, suggests that this small number is largely sufficient.

III. RESULTS AND DISCUSSION

In the regions we studied, the average kinetic energy is low enough that, on average, the particles populate the three potential wells up to a level where they differ by less than 20%, and as low as less than 2.2% for V_{LJ} and V_{12} . We also note that our energy range is low compared to standard FPU simulations.^{2,3}

After the initial transient, the time average length of the chain is computed and denoted by L . The thermal expansion of the chains with V_{LJ} , V_{11} , and V_{12} are compared in Fig. 1, where $\log(L/L_0)$ is plotted against $k_B T$. The interaction potentials have the proper asymmetry around R_0 , so the average length of the chain grows with increasing temperature. The slope $\alpha_T = (1/L)dL/dT$ identifies the coefficient of thermal expansion. Only V_{LJ} leads to an increase at high temperatures.

So far, L is also the length at which the average force exerted by the second-to-last particle on the N th particle vanishes, on average. If we fix the total length L' to be slightly smaller (larger) than L , the second-to-last particle reacts by exerting a cumulative positive (negative) average force on the last particle. We monitor this force. For small elongations and contractions, our simulations reveal a linear regime expressed by $F = E\Delta L/L$, relating the force exerted on the chain’s edge by an external force to the elongation $\Delta L = L' - L$. E is the modulus of elasticity. The estimation of the slope allows us to extrapolate E consistently from the purely mechanical behavior of the chain: this approach differs from taking advantage of thermodynamic relations and ensemble theory.^{6,7}

To estimate E , we performed averages over samples of five elements each, with varying random initial conditions, for any given pair $(T, \Delta L)$. We observed linear responses as shown in

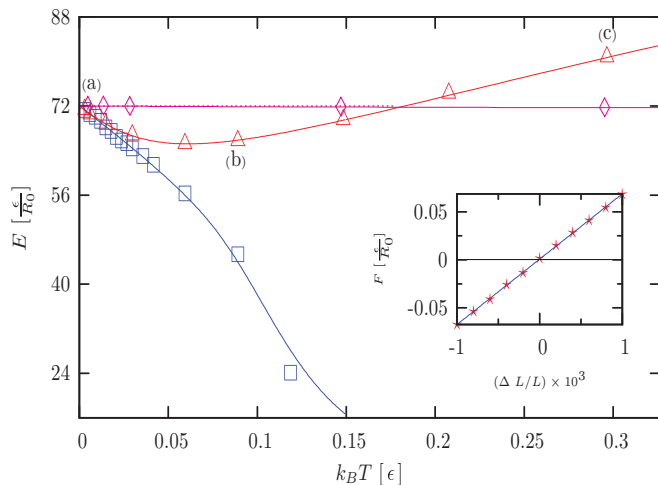


FIG. 2. (Color online) Modulus of elasticity as a function of temperature with Nosé-Hoover thermostat for V_{t1} , V_{t2} , and V_{LJ} (the symbols are as in Fig. 1). The solid lines are evaluated according to Eq. (7). The curvature change for V_{LJ} theory marks the onset of unstable effects. The dashed line refers to a chain of purely harmonic oscillators. The points (a), (b), and (c) for the case V_{t2} are referred to in Fig. 3. Inset: Example of the calculated Hooke's law constant.

the inset of Fig. 2. One data point for E entails 55 simulations in excess of 10^9 time steps.

Figure 2 shows the linear and monotonically decreasing behavior of E with increasing temperature, in qualitative agreement with most solids,^{10,16} obtained with the LJ potential. Therefore, a realistic potential of interaction, with proper short-ranged infinite repulsion and long-ranged finite attraction, is crucial but also sufficient to reproduce general properties of solids, even in one dimension [the high- T trend expressed by Eq. (1)]. There is also a point at which linearity ceases, with a net decrease in the rate of change of E . This feature has been observed in polycrystalline ceramics,^{18–20} where it is attributed to grain boundaries softening and sliding. As mentioned earlier, the chain becomes unstable if the temperature rises above some value. When this happens, we pinpoint the rest length of the chain, recursively locating the coordinate of zero average force. This extends our results. In the case of V_{t1} , E is almost constant at low temperatures and slightly increasing at high temperatures (see Fig. 2). In the case of V_{t2} , an initial decrease is followed by an inversion. These behaviors differ from what predicted by Eq. (1). Notably, E for V_{t2} and V_{LJ} starts to separate when, on average, the particles populate the two potential wells where they differ by less than 0.2%. Thus, the observed differences in the thermomechanical properties are due to seldom-sampled energy levels.

Assuming that the system is canonically distributed, the behavior in Figs. 1 and 2 can be derived exactly for any confining potential such as V_{t1} and V_{t2} . The method for the calculation echoes one that leads to the estimation of the isobaric-isothermal partition function in related models, as can be found, for example, in [Ref. 21], with the force here replacing the role of the pressure. Thus, for a fixed length \mathcal{L} and dropping the N -dependent kinetic contribution, the number of available microstates is proportional to $Z_N(\mathcal{L}, T) = \psi * \psi * \dots * \psi(\mathcal{L})$, where the $*$ denotes the Laplace convolution

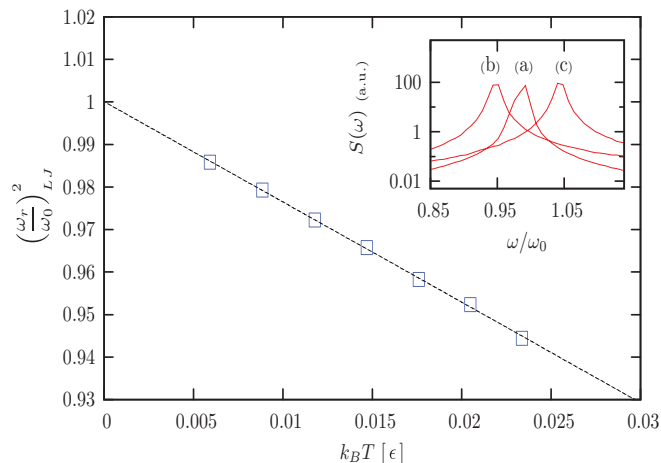


FIG. 3. (Color online) Main plot: Ratio $(\omega_r/\omega_0)^2$ with varying temperatures for the LJ model, for constant energy simulations (i.e., no thermostat). ω_0 is the extrapolated resonance frequency of zero temperature. The straight line is an interpolation. The plotted range corresponds to the linear behavior of E shown in Fig. 2. Inset: Main peak in the frequency spectra of V_{t2} canonical simulations, corresponding to the points marked (a), (b), and (c) in Fig. 2. The inversion seen in Fig. 2 is reproduced, with the resonance frequency being measurably larger when Young's modulus is larger. Spectra are normalized with arbitrary constants for comparison.

product (iterated N times) and $\psi(r) = \exp[-W(r)/(k_B T)]$. Conversely, a constant force F applied on the right edge equates to adding a potential term $-FL$, the number of microstates becoming proportional to

$$P_N(F, T) = \int_0^\infty e^{-F\mathcal{L}/(k_B T)} Z_N(\mathcal{L}, T) d\mathcal{L} = j_0(F/(k_B T))^N,$$

$j_k(z) = \int_0^\infty r^k e^{-zr} \psi(r) dr$. Hence the average length is

$$L(F) = [P_N(F, T)]^{-1} \int_0^\infty \mathcal{L} e^{-F\mathcal{L}/(k_B T)} Z_N(\mathcal{L}, T) d\mathcal{L}. \quad (5)$$

Thus, $L(F) = -N j_0'(z)/j_0(z)|_{z=F/(k_B T)}$, and

$$L = L(0) = N j_1(0)/j_0(0). \quad (6)$$

This, with $L_0 = NR_0$ and via numerical integration, leads to the results for the thermal expansion reproduced in Fig. 1. For small F , $L(F) \simeq L(0) - L(0)F/E$ and therefore $L(0) = -E \partial L / \partial F|_{F=0}$. Thus,

$$E = \frac{k_B T j_0(0) j_1(0)}{j_2(0) j_0(0) - j_1(0)^2}, \quad (7)$$

with the results in Fig. 2.²²

For the case of the LJ potential, all $j_k(0)$ diverge. Indeed, L is infinite in the thermodynamic limit for the open chain, behaving like a gas of clustered particles if $t \rightarrow \infty$. This reflects the absence of a pure crystal phase in short-ranged one-dimensional models. Unlike in three dimensions, the bulk fluctuations are of the same order as those at the boundary. Nonetheless, the metastable order is long lived at low temperatures, as confirmed by our simulations, and an approximate solution can be attempted using the same calculations as before, taking $j_k(0) = \int_0^R r^k \psi(r) dr$, with

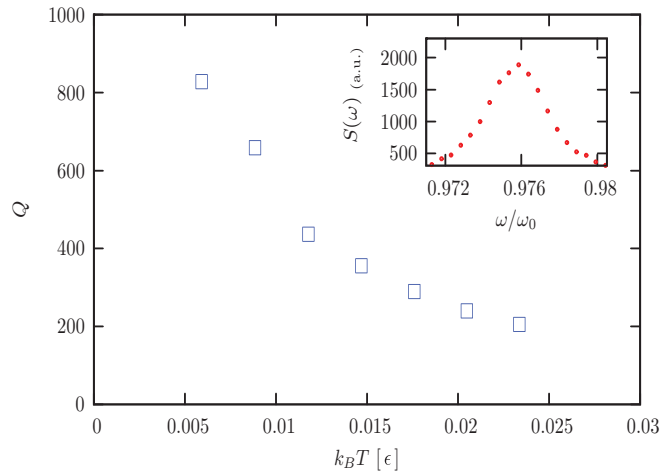


FIG. 4. (Color online) Main plot: Quality factor Q with varying temperatures for the LJ model, for constant energy simulations. Inset: Sample frequency spectrum around the main resonance, in linear scale, used to compute Q from the full width at half maximum.

$R_0 \ll R \ll R_0 e^{\epsilon/(k_B T)}$. This mimics a hard barrier preventing any two neighboring particles from exceeding separation R , in those rare instances when they otherwise would. In Figs. 1 and 2, the results agree with this theoretical analysis. The region in which E becomes sensitive to R is also visible.

We then analyzed the frequency spectrum of the position of the free end (the spectrum of the length fluctuations). We performed simulations with no bath, hence at constant energy, as in an isolated system. In the LJ case, the square of the resonance frequency ω_r decreases approximately linearly with T , in a range in which E also decreases linearly (Fig. 3, main plot). The inset of Fig. 3 shows the change of resonance frequency with T , in the V_{12} case: this variation is enslaved to the change of the elastic modulus shown in Fig. 2. This indicates that simulations with and without a thermostat are consistent as far as elastic responses are concerned.

With the LJ interaction, we investigated what we shall call the Q factor of the chain, a quantity of experimental relevance but seldom investigated in FPU models. We compute the Q from the full width at half maximum (FWHM) of the first resonance of the power spectrum of the chain length computed via constant-energy simulations. Q is thus the ratio between ω_r and the FWHM. Figure 4 shows the behavior of Q as a function of the kinetic temperature $k_B T$ (here an averaged quantity). The observed decrease with T is in qualitative agreement with experimental data for many solids. Note that here the change in Q is not the reflection of dissipation toward a bath, because the system is isolated, but is an intrinsic property of the chain due to the distribution of the energy between the fundamental mode of vibration and the other modes.

IV. CONCLUSIONS

To summarize, the thermomechanical properties of our models have been compared with those of crystalline solids via theory and simulations. The shape of the interparticle potential in the high-energy range determines the thermomechanical properties evaluated at lower average energies. Thus, the case of V_{11} and V_{12} systematically lead to an improper thermomechanical response of the chain. Realistic interaction potentials guarantee better qualitative agreement with solids' mechanical behavior. Whether these considerations are also relevant to the issue of dynamical relaxation and ergodicity is an open question.

ACKNOWLEDGMENTS

The research leading to these results has received funding from the European Research Council under the European Community's Seventh Framework Programme (FP7/2007-2013) / ERC grant agreement no. 202680. The EC is not liable for any use that can be made of the information contained herein.

*paolo.degregorio@polito.it

¹E. Fermi, J. Pasta, S. Ulam, Los Alamos Document LA-190 (1955).

²S. Lepri, R. Livi, and A. Politi, *Phys. Rep.* **377**, 1 (2003).

³A. Dahr, *Adv. Phys.* **57**, 457 (2008).

⁴*The Fermi-Pasta-Ulam Problem: A Status Report*, edited by G. Gallavotti (Springer, Berlin, 2007).

⁵D. C. Rapaport, *The Art of Molecular Dynamics Simulation*, 2nd ed. (Cambridge University Press, Cambridge, 2004).

⁶H. C. Andersen, *J. Chem. Phys.* **72**, 2384 (1980).

⁷M. Parrinello and A. Rahman, *Phys. Rev. Lett.* **45**, 1196 (1980); *J. Chem. Phys.* **76**, 2662 (1982).

⁸A. A. Berezin, A. R. Karimov, S. A. Reshetnyak, and V. A. Shcheglov, *J. Russ. Laser Res.* **23**, 381 (2002).

⁹G. K. White and M. L. Mingos, *Int. J. Thermophys.* **18**, 1269 (1997).

¹⁰H. M. Ledbetter, *Cryogenics* **22**, 653 (1982).

¹¹J. B. Wachtman Jr., W. E. Tefft, D. G. Lam, and C. S. Apsten, *Phys. Rev.* **122**, 1754 (1961).

¹²R. G. Munro, *J. Res. Natl. Inst. Stand. Technol.* **109**, 497 (2004).

¹³Y. P. Varshni, *Phys. Rev. B* **2**, 3952 (1970).

¹⁴O. L. Anderson, *Phys. Rev.* **144**, 553 (1966).

¹⁵M. L. Nandanpawar and S. Rajagopalan, *J. Appl. Phys.* **49**, 3976 (1978).

¹⁶M. X. Gu, Y. C. Zhou, L. K. Pan, Z. Sun, S. Z. Wang, and C. Q. Sun, *J. Appl. Phys.* **102**, 083524 (2007).

¹⁷M. Born and K. Huang, *Dynamical Theory of Crystal Lattices* (Oxford University, New York, 1954).

¹⁸C. Barry Carter and M. Grant Norton, *Ceramic Material* (Springer, New York, 2007), p. 53.

¹⁹E. Sánchez-González, P. Miranda, J. J. Meléndez-Martínez, F. Guiberteau, and A. Pajaresa, *J. Eur. Ceram. Soc.* **27**, 3345 (2007).

²⁰S. S. Sternstein, C. D. Weaver, and J. W. Beale, *Mater. Sci. Eng. A* **215**, 9 (1996).

²¹M. E. Fisher and B. Widom, *J. Chem. Phys.* **50**, 3756 (1969).

²²In the case of interaction potentials which depend on the nearest-neighbors coordinate difference, the Fourier convolution product replaces the Laplace convolution product, and the lower bounds in the integrals defining the j_k are extended to $-\infty$. However, within the window of our target temperatures, this does not make a noticeable difference for the calculation.